Cellular Responses of Hepatocytes Induced by Hypothermia: Modulation of Cytokinesis and Drug Metabolism-Related Functions

Audrey Legendre, Marie-José Fleury, Ilaria Allora, Marie Naudot, Thibault Bricks, Sébastien Jacques, Eric Leclerc

TITLE

Cellular responses of hepatocytes induced by hypothermia : modulation of cytokinesis and drug metabolism related functions

RUNNING HEAD

Cellular responses of hepatocytes induced by hypothermia

Audrey Legendre[1*], Marie-José Fleury[1], Ilaria Allora[1], Marie Naudot[1], Thibault Bricks[1], Sébastien Jacques[2] and Eric Leclerc[1*]

[1] CNRS UMR 7338, Laboratoire de Biomécanique et Bio ingénierie, Université de Technologie de Compiègne, France

[2] INSERM U1016 Plate-forme génomique institut Cochin, 22 rue Méchain, 75014 Paris, France

*Correspondence should be addressed to

Eric Leclerc

CNRS UMR 7338, Laboratoire de Biomécanique et Bioingénierie, Université de Technologie de Compiègne, France

Email: eric.leclerc@utc.fr

Phone: 33 (0)3 44 23 79 43

SUMMARY

Mild hypothermia is largely used in medical applications but few studies are available on this effect on drug metabolism of hepatocytes. Rat primary hepatocytes were cultured at 37°C or 32°C during 24 or 48h thanks to our Integrated Dynamic Cell Cultures in Microsystem (IDCCM) device. Although no apoptosis was detected in both temperature cultures, hepatocytes remained better differentiated until the end of the perfusion in hypothermic culture. A modulation of their ploidy was observed in response to hypothermia by enhancing the cytokinesis of multiploidic hepatocytes. RTqPCR analysis revealed a time-dependent and temperature sensitivity of the expression of several drug-metabolism related genes (*CYP1A2*, *CYP3A2, CYP2B1*, *CYP2D2, CYP2E1, GSTA2*, *UGT1A6, ABCB1b* and *ABCC2*). Whereas CYP1A2 activity remained lower in hypothermic cultures, hepatocytes remained inducible by prototypical inducers (3-methylcholentrene, rifampicin). *ABCB1* expression was upregulated by hypothermia suggesting the inefficiency of rifampicin observed during drug treatment of critical care patients. Together, these results suggest new insights on the effects of hypothermia on cellular functions and this impact on drug response of hepatocytes. Further experiments with clinically relevant drug-related CYP450 (CYP3A, CYP2C, CYP2D) could be performed in order to have a clinical relevance with therapeutic hypothermia.

Key words: mild hypothermia; hepatocytes; rat; drug metabolism ; CYP450; cell cycle

Abbreviations: Integrated Dynamic Cell Cultures in Microsystems (IDCCM), Cytochrome P450 (CYP450), 3-methylcholentrene (3MC), rifampicin (RIF)

1. INTRODUCTION

Hypothermia is a medical term that defines a situation in which there is a drop in body core temperature below 35°C. Hypothermia may be a physiological situation observed in individuals exposed to extreme environmental conditions, such as, polar explorers, mountaineers and swimmers. Mild hypothermia is defined when the body temperature is between 35 and 32°C and severe hypothermia results to a body temperature drop below 32°C. Particularly, mild therapeutic hypothermia is clinically acceptable and frequently deliberately used during surgical procedures in humans (Vaquero and Butterworth 2007) and animals (Iwata, Inoue et al. 2003). The use of therapeutic hypothermia has largely demonstrated this advantage to decrease the mortality and to improve neurological outcomes in post cardiac arrest adult patients and in neonates with hypoxic-ischemic encephalopathy (Zhou and Poloyac 2011). Mild hypothermia is clinically used in order to obtain a best conservation of the organ in the way of transplantation. Previous works have shown beneficial effects in experimental models of acute liver failure (Vaquero, Belanger et al. 2007) and of ischemia injury liver in lean and obese rats (Choi, Noh et al. 2005; Niemann, Choi et al. 2006). Indeed, mild hypothermia during hepatic ischemia helped to preserve normal liver histology, minimized the extent of necrosis, and prevented metabolic abnormalities (Niemann, Choi et al. 2006; Kuboki, Okaya et al. 2007). Particularly, the effects of hypothermia on drug disposition, metabolism and response suggest more interests to understand the altered metabolism and increased concentrations of certain drug treatments on ill patients treated by hypothermia (Tortorici 2007). The cytoprotective effects of mild hypothermia were studied for several decades but temperature sensitivity of many enzymes and drug transporters involved in drug adsorption, distribution and metabolism were rarely investigated (Zhou and Poloyac 2011).

Previously cited in vitro works were performed in traditional culture plates. Nevertheless, other culture systems are available but the loss of metabolic activity of primary hepatocytes during the culture is a recurring problem and dependent on each culture condition (Richert, Binda et al. 2002; Tuschl and Mueller 2006; Hewitt, Lechø n et al. 2007). Our laboratory developed microfluidic biochips which create a specific cell microenvironment to enhance tissue properties and toxicological assessment (Prot, Bunescu et al. 2012; Prot and Leclerc 2012). Studies were performed with hepatocytes

78 (rat/human primary cells or HepG2/C3A cell lines) cultivated in biochip alone or in our parallelized
79 biochips (named “Integrated Dynamic Cell Cultures in Microsystems” (IDCCM)) which enhanced
80 their hepatic activities (gene expression, CYP activity, albumin secretion) in comparison to static
81 cultures (Prot, Aninat et al. 2011; Baudoin, Alberto et al. 2012; Baudoin, Alberto et al. 2013; Baudoin,
82 Prot et al. 2013; Legendre, Baudoin et al. 2013). Particularly, we studied the effects of various flow
83 rates and cell densities on the level of gene expression implicated in detoxification and we performed
84 metabolic characterization (gene expression, activity) of hepatocytes cultivated in IDCCM (Baudoin,
85 Alberto et al. 2013; Legendre, Baudoin et al. 2013). These studies confirmed the maintenance of
86 primary hepatocytes in differentiation state which is a major requirement to achieve physiological
87 metabolism and toxicity during in vitro studies (Guillouzo 1998) and validated the use of IDCCM to
88 investigate drug metabolism of rat hepatocytes functions (Baudoin, Legendre et al. 2013).
89 This study was specifically designed to examine the effects of hypothermia *per se* on
90 primary rat hepatocytes cultivated in an innovative culture tool. According to therapeutic
91 hypothermia used in clinical applications (32-34°C for 12-24 hours in adults and up to 48-72
92 hours for pediatric patients) (Tortorici 2007), we fixed these two determinant parameters : the
93 culture temperature at 32°C and the time of perfusion culture at 72h (96h of culture with the
94 24h of adhesion phase). Our goal was to investigate the effect of hypothermia (32°C) on the
95 following: differentiation state (morphology, cell cycle analysis), hepatocellular performance
96 (albumin secretion, glucose consumption), metabolic activity and liver-related gene
97 expressions.
98

2 . MATERIALS AND METHODS

2.1 Primary rat hepatocyte culture in IDCCM

The experiments were performed during 5 days. It included three phases: the day of hepatocyte extraction (*Day 0*), the adhesion phase (*Day 1*) at 37°C and 72h of perfusion phase (*from Day 2 to Day 4*) at 37°C or 32°C.

2.1.1 Primary rat hepatocyte isolation

Primary hepatocytes from 5-week-old male Sprague-Dawley rats (*rattus norvegicus*) weighing about 200-250g were isolated by a modification of the two-step *in situ* collagenase perfusion according to the method of Seglen (Seglen 1973). Animals were provided by the Janvier Elevage Animal Center (Le Genest Saint Isle, France). They were housed at the University of Compiegne with a 12h light / dark cycle at 22°C with food and water *ad libitum*. All experiments were approved by the Animal Experimental Committee of the University of Compiegne. The animal was anesthetized by intra peritoneal injection of sodium pentobarbital (Centravet, Gondrevrille, France). Briefly, after *in situ* washing and perfusion with collagenase solution (Fisher Scientific, Illkirch, France) at 30ml/min, the liver was extracted and the digested liver tissues were filtered through cotton gauze, then 400 and 100µm filters. The cell suspension was centrifuged and washed three times. Percoll isogradient centrifugation was performed to discard dead cells and a significant portion of the non-parenchymal cells. The resulting cells were finally suspended in the culture medium as described below. Cell viability was assessed by trypan blue dye exclusion and hepatocytes with a viability of greater than 90% were used.

Freshly isolated hepatocytes were cultured in first 24 hours in seeding medium composed by William's E GLutamax medium (Fisher Scientific) supplemented with bovine

insulin (5µg/ml, Sigma-Aldrich, Saint-Quentin Fallavier, France) and fetal bovine serum (10%). To enhance cell adhesion, the inner surface of the biochips was coated with rat tail type 1 collagen (0.3mg/ml, Becton Dickinson, Biosciences, Le Pont de Claix, France) prepared in phosphate-buffered saline (PBS, Fisher Scientific) for 1 hour at 37°C in a humidified atmosphere supplied with 5% CO_2. After washing with seeding medium, the cells were inoculated at a density of 0.5×10^6 cells per biochip (0.25×10^6 cells per cm²) inside the biochips and incubated with seeding medium at 37°C, 5% CO_2. After 24 hours, cells were cultured in William's E GLutamax medium supplemented with 3mg/ml Bovin Serum Albumin (Sigma-Aldrich), 5ng/ml dexamethasone (Sigma-Aldrich), 6.25µg/ml insulin-transferrin-selenium solution (BD Biosciences), 100units/ml penicillin and 100mg/ml streptomycin (Fisher Scientific).

2.2.2 Dynamic culture in microfluidic biochips of IDCCM

The entire set up was called the IDCCM for "Integrated Dynamical Cell Culture in Microsystems". The concept of the IDCCM box is presented in detail in our previous work (Baudoin, Alberto et al. 2012). Briefly, the biochips are made in polydimethylsiloxane (PDMS) conventional moulding (**Figure 1A-C**) according to homemade design (Baudoin, Griscom et al. 2011; Baudoin, Prot et al. 2013). After cell adhesion, perfusion of IDCCM was performed thanks to polytetrafluoroethylene (PTFE) tubes which were connected to the fluidic cover of the IDCCM and to the peristaltic pump (**Figure 1D**). The entire system (pump and IDCCM) was placed into the incubator (37°C or 32°C, 5% CO_2). Perfusion started with a flow rate of 25µl/min and stopped after 72h of culture. After adhesion phase and 24h, 48h and 72h of perfusion, cytochrome assays, cell counting and viability were directly performed on biochips (see below). Culture medium was stocked at -20°C for posterior assays and cell pellets were stocked at -80°C until RNA extraction (see below).

149

150 **2.2.3 Cell counting and viability**

151 Cell counting was performed on Malassez cell after cell detachment with trypsin-
152 EDTA (Fisher Scientific). Cell viability was quantitatively analysed by trypan blue dye
153 exclusion.

154

155 **2.4 Cell morphology**

156 F-actin and nuclei staining were performed to observe cell morphology after 48h of
157 perfusion. Cells cultivated in biochips were fixed for 10 min with paraformaldehyde (4%) and
158 permeabilized in 0.1% Triton X100/ PBS for 10 min. After washing in PBS, the f-actin was
159 stained for 20 min with rhodamine-phalloidin® (Invitrogen) and nuclei were stained with
160 DAPI 2 µg/mL (Invitrogen) for 10 min. Biochips were directly observed using a conventional
161 fluorescence microscope (Leica DMI 6000B, LAS-AF software, Leica Microsystems).

162

163 **2.5 Cell cycle**

164 Trypsined cells were washed twice and centrifugated at 5,000 rpm for 5 min at 4°C).
165 Cells were fixed for 45 min with ice-cold ethanol 75% in PBS. After washing in PBS, cells
166 were suspended with a solution containing PBS, 0.1% Triton X100, 40 µg RNase A (Sigma-
167 Aldrich), and 25 µg propidium iodide (Invitrogen). After 15 min of incubation and protected
168 from light, stained samples were analyzed in an Epics XLMCL flow Cytometer (Beckman
169 Coulter, Roissy, France). Histograms were analyzed using Multicycle AV™ software (De
170 Novo Software, USA, Los Angeles).

171

172 **2.6 Albumin**

Albumin synthesis was reported as specific hepatic marker. Albumin was measured using an ELISA sandwich test in a 96-well plate according the protocol of rat albumin ELISA Quantitation Set (Bethyl Laboraries, Euromedex, Souffelweyersheim, France). Briefly, albumin concentration of medium samples was analyzed in triplicate, using a polyclonal antibody to rat albumin (ref. number: A110-134A and A110-134P). Standard curves were generated using purified rat albumin diluted in culture medium. Absorbance was measured by a microplate reader (Tecan, Spectrafluor plus). For each assay, curve was generated as a 4-paramater curve fit using MasterPlex ReaderFit (Hitachi Solutions America, Ltd, MiraiBio Group (2012), available from www.readerfit.com).

2.7 Glucose

In order to assess cell activity, glucose consumption was analyzed using a biochemical analyzer, the Konelab 20 (Thermo Fisher Electron Corporation, Courtaboeuf, France). Two different steps were involved in the reaction: the transformation of glucose in H_20_2 and D-gluconate by the glucose oxidase, and then the transformation of H_20_2 in quinone imine by the peroxidase. The absorbance of quinone imine is measured at a wavelength of 510nm.

2.8 Cytochrome 1A2 assay

Metabolic performance of hepatocytes was performed with CYP1A2 activity Activity was determined using 5-ethoxyresorufin (10µM) as substrate. Resorufin formation by 7-ethoxyresorufin O-deethylation was quantified by a fluorescence micro-plate reader (TECAN, Spectrafluor plus) after 1 hour incubation at 32 or 37°C, CO_2 5% in the presence of salicylamide (3mM) in order to inhibit phase II enzymes. Parallely, we measured both basal and induced levels of CYP1A2 activity after incubation of 3-methylchlorentrene (5µM) or

rifampicin (25µM – negative control) during 72h of perfusion. All products were purchased from Sigma-Aldrich.

2.8 Quantitative RTqPCR

Total RNA was extracted using the Nucleospin® RNA XS isolation kit (Macherey-Nagel EURL, Hoerdt, France). The quantity of RNA was assessed with a Nanodrop ND-1000 spectrophotometer (Nyxor Biotech,Paris, France). RNA qualitation was evaluated using the Agilent 2100 Bioanalyzer (using the Agilent RNA 6000 Nano and Pico kits). All RNA samples had an RNA Integrity Number of more than 8 (between 9.3 and 10). cDNA were synthesized from 500ng of total RNA with oligodT Primer, using SuperScript II (Life Technologies), according to the manufacturer's protocol.

Quantitative RT-PCR (RTqPCR) was performed using the Real Time PCR system LC480 (Roche) with the LightCycler 480 Sybr Green I Master and the LightCycler 480 Probes Master (Roche), for the housekeeping genes and the targets genes respectively. Pairs of primers for each of the 23 targets genes (**Table 1**) were designed using the Roche RealTime ready (UPL probes) Configurator tool. Couples of primers for housekeeping genes (*GAPDH*, *HPRT1*, *PPIB* and *SDHA*) were designed with Primer3, and tested for efficiency and specificity. GeNorm software application allows selecting the two most stable housekeeping genes in our model. All the couples were used in duplicate. Data from target genes were normalized with the two reference genes (*GAPDH* and *PPIB*). Data were analyzed using the ΔCt method (Pfaffl 2001) after validation of each duplicate (i.e. elimination of outliers' measures from duplicate with standard deviation above 0.4).

2.9 Statistic analysis

Three independent experiments (*i.e* 3 euthanized rats) were assessed. Each experiment was repeated at least three times in triplicate biochips except for data of RTqPCR analysis and **table 3** where experiments were repeated only twice. Data were plotted as mean ± standard deviation (SD). Statistical analyses were performed by unpaired t test using GraphPad statistical analysis (Prism 5, version 5.02). The statistically significant differences are reported on the histograms and tables (*** P<0.001, ** P<0.01, * P<0.05).

3. RESULTS

Cell morphology and viability

After 96h of cell culture in biochips (72h of perfusion), hepatocytes were refringent between their cell junctions with a typical cuboid shape and mono- or multinucleus (**Figure 2A**). Under hypothermia cell morphology was not affected as observed by phase contrast microscopy (**Figure 2B**) or by immunodetection of actin filament in the cytoskeleton (**Figure 3**). No effect was observed in induction experiments (**data not shown**).

The cell counting showed no difference on cell number per biochip between both temperatures (**Figure 4**). Only 40% of inoculated cells remained seeded on biochip (initial density at 500 000 cells / biochip) and the number slightly decreases after the first 24h of perfusion. After 72h of perfusion (Day 4), we observed that the cell number increased approximately 50% of initial cell density. No effect was observed in induction experiments (data not shown). Thanks to trypan blue staining, we detected no difference in the viability between normo and hypothermic culture (**data not shown**). Together, data evidenced that hypothermia had no effect on viability of cells cultivated in biochips.

Change of the ploidy state of hepatocytes

Cell cycle analysis demonstrated that hepatocytes stopped dividing and entered in G0 state when hepatocytes were extracted from animal (**Figure 5A**). Approximately 30 % were arrested in G0/G1 and, therefore, none dividing. G0/G1 state regrouped binucleated hepatocytes and proportion of G2/M (~ 60%) represented tetranucleated cells (**Figure 5A**). The profile observed at Day 0 was typical of differentiated hepatocytes composing liver cell population. Post extracted cell cycle profile was modified after 24h of culture in static condition at 37°C. The proportion of G0/G1 increased to ~ 40% (*p-value < 0.001*) whereas S phase remained stable (< 10%) (**Figure 5A**). The increase of the G0/G1 phase and a stable S phase illustrated the typical response of cells under microconfinement imposed by biochips during the first 24h of culture (Prot, Aninat et al. 2011; Snouber, Letourneur et al. 2012). After 24h of perfusion in hypothermia (**Figure 5C**), we observed an increase of G2 state and a decrease of S state, at ~ 60% (*p-value < 0.001*) and 5% (*p-value < 0.05*), respectively, whereas cell cycle profile remained identical between day 1 and day 2 at 37°C (**Figure 5B**). After 72h of perfusion (Day 4), an increase of G2 state was equally observed at 37°C, whereas primary rat hepatocytes cultivated in hypothermia recovered the same cell cycle profile than cells at Day 2-37°C (**Figure 5B & C**). During all the time of culture, no sub G1 cells were detected in hepatocyte cultures confirming that dead cells counted with trypan blue dye exclusion was not in apoptosis (**Figure 5**). In induction experiments, we detected rifampicin effect on G0/G1 and G2 state which concerned near 45% of total population, for each state (however statistical analysis reveals a high *p-value*, *P>0.01*). This effect was independently of temperature (**Figure 5B & C**). No effect was observed in 3-methylchlorentrene induction experiments (**Figure 5B & C**).

Hepatocellular performance in hypothermic culture

Hepatocellular performance was evaluated during the 96h of culture in induced and uninduced culture. Glucose consumption was not modified by hypothermia except after the first 24h of perfusion where consumption was higher in 37°C (124 ± 34.2 µg/10^6 cells/hour) than in 32°C (77.2 ± 6.1 µg/10^6 cells/hour) (*p-value < 0.01*) (**Figure 6A**) . No difference was observed in induction experiments in comparison with uninduced culture and regarding temperature (**Figure 6A**). Specific cell activity was also studied in hypothermia culture regarding albumin secretion (**Figure 6B**). Hepatocytes secreted the same level of albumin at both temperatures except after 48h of perfusion (Day 3) where secretion continue to increase until (691 ± 247.4 ng/10^6 cells/hour) and is significantly higher (x 3.8 times) in hypothermic culture. In induction experiments, primary rat hepatocytes secreted between 4 and 5.6 times more albumin than in uninduced culture. Same induction was observed after 3-methylchlorentrene and rifampicin inductions but it was independent of the temperature (**Figure 6B**). These results confirm that inducers were used at non cytotoxic concentration in our primary rat hepatocytes culture.

Liver related gene expressions were modulated in hypothermic culture

Thanks to RTqPCR analysis, we evaluated some liver related gene expressions (hepatic transcription factors, xenosensors, CYPs, phase II metabolism enzymes, ABC transporters and stress-related genes) of primary rat hepatocytes cultivated at 37 or 32°C. We compared these expressions after the first 24h of perfusion (**Figure 7A**) and at the end of culture (72h of perfusion) (**Figure 7B**) in comparison with the post extraction levels. After 24h (Day 2) and 72h (Day 4) of perfusion, PXR target genes (*CYP3A23/3A1, GSTA2, UGT1A6, ABCB1b)* and oxidative stress related genes (*HMOX1, NQO1*) were induced at least above 50% of the post extraction levels at both temperature. We found a higher expression for genes related to phase I metabolism (*CYP1A2*, *CYP3A2, CYP2B1*, *CYP2D2* and *CYP2E1* at

Day 2 in hypothermic culture but their levels are lower at Day 4. Phase II enzymes (*GSTA2*, *UGT1A6*) and oxidative stress related genes (*HMOX1, NQO1*) remained upregulated between day 2 and day 4. Furthermore, they were more induced in hypothermia at Day 4 *versus* Day 2 ($p\text{-value} < 0.01$) (**Figure 7B**). Inversely, *SULT1A1* expression was the only gene which was inhibited by hypothermia overtime in the culture.

A complex regulation of CYP1A2 in hypothermic culture

We checked the effect of temperature culture on basal activity of CYP 1A2 in primary rat hepatocytes. CYP1A2 activity of uninduced culture is higher (x 3 times) at 37°C in comparison with hypothermic culture (**Figure 8A**). This difference was significant after 24 and 72h of perfusion. In order to detect if the difference between both temperatures is also observed in traditional plate culture, we compared the data at the Day 2 of the culture, when the effect of hypothermia on CYP1A2 activity was detected in IDCCM cultures (**supplemental data, table 3**). First, we observed the same effect of hypothermia on primary rat hepatocytes in plates. Second, we confirmed the capacity of IDCCM culture to enhance (x 22 times or x 11 times, at 37°C and 32°C, respectively) the hepatic performance (CYP1A2 activity) of primary rat hepatocytes when compared to plates.

After 3-methylchlorentrene exposure, the inductibility of both cultures was confirmed but hypothermic cultures were more inducible (fold change ~ 4.5 at 32°C *vs* ~ 2 at 37°C) (**Figure 8B**). This led to equalize the resorufin production by the CYP1A2 to 3000±500 pmol/h/10^6 cells and to 3100±200 pmol/h/10^6 cells at 37°C and 32°C respectively. The levels of the mRNA after 72h of induction by 3-methylchlorentrene (**Table 2**) were also compared to uninduced culture (at 37 or 32°C). As expected, we observed an upregulation of *AhR* and their related genes (*CYP1A2, GSTA2* and *UGT1A6).* Whereas *AhR* was lower induced by 3MC in hypothermic culture, *CYP1A2* expression was induced at the same level at both

cultures as observed for CYP1A2 activity. Temperature sensitivity of phase 2 enzymes (*GSTA2* and *UGT1A6)* was different with a higher induction (x2) of their expressions at 32°C.

According to our attempt, the negative control, rifampicin (CYP3A4 inductor) was not able to induce CYP1A2 activity at both temperatures (**Figure 8B**). mRNA analysis confirmed the expected upregulation of PXR (higher than with 3-methylchlorentrene induction) and their target genes in normo and hypothermia (**data not shown**). Interestingly, we observed that *ABCB1b* expression was more induced in hypothermic culture (x4) than in normothermic culture.

4. DISCUSSION

Cytoprotective effect of hypothermia is largely reported (Lampe and Becker 2011) but regarding hepatocytes, few studies are available on the hepatic performance when they are cultivated in new *in vitro* microfluidic tools. The mechanisms induced by hypothermia suggest new insights in medical interests as acute liver failure treatment (Sundaram and Shaikh 2011) and liver transplantation (Gurusamy, Gonzalez et al. 2010). Nevertheless, some medical cases reported a modulation of drug disposition, metabolism, and response of hepatocytes in patients treated by hypothermia (Zhou and Poloyac 2011). Changes in metabolic activity of hepatocytes could result in adverse drug events in patients and therefore became a negative secondary effect (Tortorici 2007). In order to investigate these phenomena, we focused our study on hepatocellular performance, metabolic activity and liver related gene expressions. We designed the experiments to compare normo (37°C) and hypothermic (32°C) culture of hepatocytes cultivated during 72h in perfusion inside our microfluidic tool, the IDCCM. These parameters were chosen according to therapeutic hypothermia used in clinical applications employed at 32-34°C for 12-24h in adults and up to 48-72 h for pediatric patients (Tortorici 2007).

We used our new microfluidic tools to study the effects of hypothermia on primary rat hepatocytes. The potential of IDCCM permits to enhance hepatocyte phenotype and sensitivity closer to *in vivo* level (Baudoin, Alberto et al. 2013; Legendre, Baudoin et al. 2013). For example, thanks to PDMS, beneficial diffusion of the O_2 and CO_2 is created which is necessary for detoxification of primary rat hepatocytes (Schmitmeier, Langsch et al. 2006). This enhanced oxygenation permits to increase CYP1A2 activity which is higher in IDCCM than in traditional cultures (supplemental data, table 3). However, our approach still faced some limitations due to the complexity of the IDCCM microfluidic tool by comparison to the conventional culture methods (including biochip manipulations, number of replicates when compared to 96 well plates and the subsequent variability; type of microfluidic tools leading to variability lab-to-lab users, lack of comparative literature data). Nevertheless, our study demonstrated that primary rat hepatocytes cultured in hypothermia in IDCCM conserved characteristics of non-activated (limited proliferation), functional and differentiated hepatocytes as observed for hepatoblastoma cells in culture plates (Kosovsky, Khaoustov et al. 2000). Primary rat hepatocytes cultured at normo and hypothermia exhibit characteristics of functional and differentiated hepatocytes as illustrated by albumin secretion, the liver-specific marker (Reid and Jefferson 1984). In contrast with other studies performed in traditional culture plates (Katsuki, Kurosawa et al. 2004) (Fu, Blei et al. 2004), no inhibition of albumin secretion and no apoptosis were observed after short-term mild hypothermia in primary rat hepatocytes cultivated in our microfluidic tools. ~~In contrast with the study of Katsuki *et al.* performed in coated plates, no inhibition of albumin secretion was observed in primary rat hepatocytes after short term mild hypothermia (Katsuki, Kurosawa et al. 2004). Albumin secretion attempted its maximal value after 48h of perfusion in hypothermic culture against 24h of perfusion in 37-cultured hepatocytes. After 72h of perfusion, albumin secretion was reduced in both cultures. This oscillation has been already measured in short culture of~~

hepatocytes in microfluidic tools (Kane, Zinner et al. 2006; Toh, Lim et al. 2009). Regarding viability, no apoptosis was observed with cell cycle analysis at both temperatures. This observation is not in agreement with the data obtained in primary mouse hepatocytes cultivated in traditional culture plates (Fu, Blei et al. 2004).

Adult liver is a quiescent organ, but it can retain a capacity to proliferate and to modulate its ploidy in response to various stimuli or aggression (partial hepatectomy, metabolic overload (i.e., high copper and iron hepatic levels), oxidative stress, toxic insult, and chronic hepatitis etc.) (Gentric, Desdouets et al. 2012). Our cell cycle analysis confirmed the differentiated state of primary rat hepatocytes thanks to their typical profiles already reported for rat (Gerlyng, Stokke et al. 2005) / mouse primary cells (Fu, Blei et al. 2004) or hepatoma-derived cells (Sainz and Chisari 2006). Indeed, primary rat hepatocytes are not in proliferation (no increase of S phase) and they can be diploid (2N), tetraploid (2 x 2N, 4N), or octoploid (2 x 4N, 8N) (and a few even hexadecaploid) which each distribute through the different phases of the cell cycle (Gerlyng, Stokke et al. 2005). Effect of hypothermia was observed particularly after the first 24h of perfusion when the proportion of G2 cells increases whereas S cells decrease. The same phenomenon was observed after 72h of perfusion in normothermic culture. These data are linked to a modification of the ploidy state of hepatocytes in biochips which seem to appear earlier in hypothermic culture. Thanks to microarray analyse, Sonna *et al*. show an induction of many genes implicated in cell cycle and cell division of HepG2 cells in hypothermia which could be explained our flow cytometry results (Sonna, Kuhlmeier et al. 2010). In addition, the reduction of ploidy could equally explain the increase of cell number (by cytoplasmic split) observed after 72h of perfusion in normo and hypothermic culture. Recently, this phenomenon, named “the concept of ploidy conveyor”, was described by Duncan *et al*. as the capacity of hepatocytes to increase (failed cytokinesis) and reduce (multipolar mitosis) their ploidy (Duncan, Taylor et al. 2010). More

investigations are necessary to explain the cell function of these ploidy state modulations when cells are in hypothermia. ~~Rifampicin induction also modified ploidy profile of primary rat hepatocytes cultivated in biochips equilibrating the proportion of G0/G1 and G2 at 50%. This effect remained independent of temperature. Regarding the work of Zhuang et al. which suggest the role of PXR in the cell cycle arrest of HepG2 (Zhuang, Jia et al. 2011), our data suggest that rifampicin (used at non cytotoxic effect) could modify cell cycle of primary rat hepatocytes *via* the PXR pathway. More investigations are also necessary to explain the cell function of these ploidy state modulations when cells are in hypothermia.~~

Complex regulation of gene expression was evidenced in our study. Particularly, sensitivity to hypothermia was not the same after 24h and 72h of perfusion. First, we detected that hypothermia induced most of selected genes after 24h in hypothermic culture (48 % of the analysed genes versus 30% after 72h), confirming a time-dependent sensitivity. Expressions of some CYPs (*CYP1A2*, *CYP3A2, CYP2B1*, *CYP2D2* and *CYP2E1)* were higher after 24h than in normothermic culture, whereas they were lower after 72h. Phase II enzymes expressions (*GSTA2*, *UGT1A6*) increased from 24 to 72h of culture and remained higher in hypothermic culture. The level of ABC transporters were upregulated by hypothermia only after 72h of perfusion. Together, these results suggest time-dependent and temperature sensitivity of CYPs, phase II metabolism enzymes and ABC transporters. As reported in human liver microsomes (Tortorici 2007), we demonstrated with our biochips that mild hypothermia may produce isoform specific alterations of CYP450-mediated expression and metabolism. Some studies reports that hypothermia alters multiple aspects of enzymatic function and a potential mechanism on CYPs metabolism may be through changes in the binding pocket information (Tortorici 2007; Zhou and Poloyac 2011). Moreover, we reported that temperature-sensitivity of hepatocytes may be different on the RNA transcription level and on the enzymatic activity (for example, CYP1A2). CYP1A2 activity assay evidenced that

the level of basal activity in lower in hypothermic culture from 24h of perfusion. ~~Beyond to confirm the potential of inducibility of rat hepatocytes in IDCCM by prototypical inducers, inductive experiments with 3-methylchlorentrene evidenced that hypothermic hepatocytes remain inducible. Precisely, the level of *CYP1A2* mRNA was induced at the same way at both temperatures in order to equalize CYP1A2 activity in hypothermic and normothermic culture.~~

The temperature-sensitivity observed on *CYP1A2*, *CYP3A2*, *CYP2E1*, *CYP2C*, *CYP2C6*, *CYP2D1* and *CYP2D2* expression levels could explain the reduction of metabolism in hypothermia treated patients (Zhou and Poloyac 2011) (Martignoni, Groothuis et al. 2006; Grobe, Kutchan et al. 2012) and evidenced the importance of the duration of hypothermia. Indeed, a lot of these CYPs are implicated in the metabolism of commonly used drugs in critical care patients. Besides to be a prototypical inducer of PXR pathways (Lu and Li 2001; Lin 2006), rifampicin is an antimicrobial commonly used drugs in critical care patients. Rifampicin (also named rifampin) is known to be a substrate per se and to interact with drugs that are substrates for P-glycoprotein efflux pump, the product of *ABCB1* gene (Zhou 2008). Some studies reported that rifampicin upregulated of P-glycoprotein in human cell lines (Schuetz, Schinkel et al. 1996) and primary rat hepatocytes cultivated in IDCCM (Legendre, Baudoin et al. 2013) under normothermia. The upregulation of *ABCB1* gene by hypothermia in comparison with normothermia could so explain the inefficiency of rifampicin and other drugs which were mainly observed during drug treatment of patients, as for example verapamil, digoxin (which are equally substrates of P-glycoprotein) (Zhou 2008). Recent works suggest also that the negative effect of hypothermia was often evidenced by the decrease of the clearance of drugs with apparently change in enzyme substrate affinity and/or in elimination route specific (Zhou, Empey et al. 2011; Zhou and Poloyac 2011).

5. CONCLUSION

Hypothermia is largely used in surgery and therapeutic medicine. Some cell mechanisms have been described but barely any information is available on the effects of hypothermia on liver. New *in vitro* tools using microfluidic technology have proved their efficiency in the improvement of hepatocyte functions. They appear more adapted to drug metabolism studies but equally to respond to the scientific requests. Using the enhancement of hepatocyte functions in IDCCM, hepatic effect of hypothermia reveals new insights for therapeutic research. We reported that the ploidy state and hepatocellular performance were sensitive to hypothermia. Time-dependent temperature sensitivity was observed, particularly on the mRNA transcription level and enzymatic/protein activity of drug metabolism actors (CYPs, phase II enzyme and ABC transporters). Negative secondary effects of hypothermia observed on metabolism of drug treated patients seem to result from complex actions of hypothermia on hepato-specific functions. Future research efforts are essential to delineate mechanisms of the effects of hypothermia on drug disposition, metabolism, and response. Particularly, the most common of drugs-related CYP450 (CYP3A, CYP2C, CYP2D) could be more analyzed in order to have a clinical relevance with therapeutic hypothermia. Furthermore, mechanisms implicated beyond hypothermia (after re-warming when the temperature increase from 32°C to 37°C) could be more investigated to understand the phenomena which take place in medical applications.

Acknowledgements & conflict of interest

This work was supported by the « Fondation pour la Recherche et l'Innovation » of University of Technology of Compiegne (France). We thank Laurent Griscom from UMR 8089 SATIE Biomis, ENS de Cachan who fabricated the mould master of the microfluidic biochips used in this study. The authors report any conflict of interest.

REFERENCES

Baudoin R, Alberto G, et al. Investigation of the levels of expression and activity of detoxication genes of primary rat hepatocytes under various flow rates and cell densities in microfluidic biochips. Biotechnology Progress 2013; in press.

Baudoin R, Alberto G, et al. Parallelized microfluidic biochips in multi well plate applied to liver tissue engineering. Sensors and Actuators B: Chemical 2012; 173 (0): 919-926.

Baudoin R, Griscom L, et al. Behavior of HepG2/C3A cell cultures in a microfluidic bioreactor. Biochemical Engineering Journal 2011; 53 (2): 172-181.

Baudoin R, Legendre A, et al. Evaluation of a Liver Microfluidic Biochip to Predict In Vivo Clearances of Seven Drugs in Rats. J Pharm Sci 2013: in press.

Baudoin R, Prot JM, et al. Evaluation of seven drug metabolisms and clearances by cryopreserved human primary hepatocytes cultivated in microfluidic biochips. Xenobiotica 2013; 43 (2): 140-152.

Choi S, Noh J, et al. Mild hypothermia provides significant protection against ischemia/reperfusion injury in livers of obese and lean rats. In: Ann Surg. United States. 2005. 241**:** 470-476.

Duncan AW, Taylor MH, et al. The ploidy conveyor of mature hepatocytes as a source of genetic variation. Nature 2010; 467 (7316): 707-710.

Fu T, Blei AT, et al. Hypothermia inhibits Fas-mediated apoptosis of primary mouse hepatocytes in culture. Cell Transplant 2004; 13 (6): 667-676.

Gentric G, Desdouets C, et al. Hepatocytes polyploidization and cell cycle control in liver physiopathology. Int J Hepatol 2012; 2012: 282430.

Gerlyng P, Stokke T, et al. Analytical methods for the study of liver cell proliferation. Cytometry 2005; 13 (4): 404-415.

Grobe N, Kutchan TM, et al. Rat CYP2D2, not 2D1, is functionally conserved with human CYP2D6 in endogenous. FEBS Lett 2012; 586 (13): 1749-1753.

495 Guillouzo A. Liver cell models in in vitro toxicology. Environmental Health Perspectives 1998; 106:
496 511-532.
497 Gurusamy KS, Gonzalez HD, et al. Current protective strategies in liver surgery. World J
498 Gastroenterol 2010; 16 (48): 6098-6103.
499 Hewitt NJ, Lechøn MaJGm, et al. Primary Hepatocytes: Current Understanding of the Regulation of
500 Metabolic Enzymes and Transporter Proteins, and Pharmaceutical Practice for the Use of
501 Hepatocytes in Metabolism, Enzyme Induction, Transporter, Clearance, and Hepatotoxicity
502 Studies. Drug Metabolism Reviews 2007; 39 (1): 159-234.
503 Iwata T, Inoue S, et al. Comparison of the effects of sevoflurane and propofol on cooling and
504 rewarming during deliberate mild hypothermia for neurosurgery. Br J Anaesth 2003; 90 (1):
505 32-38.
506 Kane BJ, Zinner MJ, et al. Liver-specific functional studies in a microfluidic array of primary
507 mammalian hepatocytes. Anal Chem 2006; 78 (13): 4291-4298.
508 Katsuki M, Kurosawa H, et al. Enhancement of albumin secretion by short-term hypothermic
509 incubation of primary rat hepatocytes. Biochemical Engineering Journal 2004; 20 (2–3): 137-
510 141.
511 Kosovsky MJ, Khaoustov VI, et al. Induction of hepatitis B virus gene expression at low temperature.
512 Biochim Biophys Acta 2000; 1490 (1-2): 63-73.
513 Kuboki S, Okaya T, et al. Hepatocyte NF-kappaB activation is hepatoprotective during ischemia-
514 reperfusion injury and is augmented by ischemic hypothermia. In: Am J Physiol Gastrointest
515 Liver Physiol. United States. 2007. 292**:** G201-207.
516 Lampe JW and Becker LB. State of the art in therapeutic hypothermia. Annu Rev Med 2011; 62: 79-
517 93.
518 Legendre A, Baudoin R, et al. Metabolic characterization of primary rat hepatocytes cultivated in
519 parallel microfluidic biochips. J Pharm Sci 2013; 102 (9): 3264-3276.
520 Lin JH. CYP induction-mediated drug interactions: in vitro assessment and clinical implications.
521 Pharm Res 2006; 23 (6): 1089-1116.

522 Lu C and Li AP. Species comparison in P450 induction: effects of dexamethasone, omeprazole, and
523 rifampin on P450 isoforms 1A and 3A in primary cultured hepatocytes from man, Sprague–
524 Dawley rat, minipig, and beagle dog. Chemico-Biological Interactions 2001; 134 (3): 271-
525 281.
526 Martignoni M, Groothuis GM, et al. Species differences between mouse, rat, dog, monkey and human
527 CYP-mediated drug metabolism, inhibition and induction. Expert Opin Drug Metab Toxicol
528 2006; 2 (6): 875-894.
529 Niemann CU, Choi S, et al. Mild hypothermia protects obese rats from fulminant hepatic necrosis
530 induced by ischemia-reperfusion. In: Surgery. United States. 2006. 140**:** 404-412.
531 Pfaffl MW. A new mathematical model for relative quantification in real-time RT-PCR. Nucleic Acids
532 Res 2001; 29 (9): e45.
533 Prot JM, Aninat C, et al. Improvement of HepG2/C3a cell functions in a microfluidic biochip.
534 Biotechnol Bioeng 2011; 108 (7): 1704-1715.
535 Prot JM, Bunescu A, et al. Predictive toxicology using systemic biology and liver microfluidic "on
536 chip" approaches: application to acetaminophen injury. In: Toxicol Appl Pharmacol. United
537 States, 2012 Elsevier Inc. 2012. 259**:** 270-280.
538 Prot JM and Leclerc E. The current status of alternatives to animal testing and predictive toxicology
539 methods using liver microfluidic biochips. Ann Biomed Eng 2012; 40 (6): 1228-1243.
540 Reid LM and Jefferson DM. Culturing hepatocytes and other differentiated cells. Hepatology 1984; 4
541 (3): 548-559.
542 Richert L, Binda D, et al. Evaluation of the effect of culture configuration on morphology, survival
543 time, antioxidant status and metabolic capacities of cultured rat hepatocytes. Toxicol In Vitro
544 2002; 16 (1): 89-99.
545 Sainz B and Chisari FV. Production of infectious hepatitis C virus by well-differentiated, growth-
546 arrested human hepatoma-derived cells. Journal of Virology 2006; 80 (20): 10253-10257.
547 Schmitmeier S, Langsch A, et al. Development and characterization of a small-scale bioreactor based
548 on a bioartificial hepatic culture model for predictive pharmacological in vitro screenings.
549 Biotechnol Bioeng 2006; 95 (6): 1198-1206.

550 Schuetz EG, Schinkel AH, et al. P-glycoprotein: a major determinant of rifampicin-inducible
551 expression of cytochrome P4503A in mice and humans. Proc Natl Acad Sci U S A 1996; 93
552 (9): 4001-4005.
553 Seglen PO. Preparation of rat liver cells. 3. Enzymatic requirements for tissue dispersion. Exp Cell
554 Res 1973; 82 (2): 391-398.
555 Snouber LC, Letourneur F, et al. Analysis of transcriptomic and proteomic profiles demonstrates
556 improved Madin–Darby canine kidney cell function in a renal microfluidic biochip.
557 Biotechnology Progress 2012; 28 (2): 474-484.
558 Sonna LA, Kuhlmeier MM, et al. A microarray analysis of the effects of moderate hypothermia and
559 rewarming on gene expression by human hepatocytes (HepG2). Cell Stress Chaperones 2010;
560 15 (5): 687-702.
561 Sundaram V and Shaikh OS Acute liver failure: current practice and recent advances. In:
562 Gastroenterol Clin North Am. United States. 2011. 40**:** 523-539.
563 Toh YC, Lim TC, et al. A microfluidic 3D hepatocyte chip for drug toxicity testing. Lab on a Chip
564 2009; 9 (14): 2026-2035.
565 Tortorici MA (2007). The effects of therapeutic hypothermia on cytochrome P450-mediated
566 metablism : studies in translational research. Doctor of Pharmacy, University of Pittsburgh.
567 Tuschl G and Mueller SO. Effects of cell culture conditions on primary rat hepatocytes-cell
568 morphology and differential gene expression. Toxicology 2006; 218 (2-3): 205-215.
569 Vaquero J, Belanger M, et al. Mild hypothermia attenuates liver injury and improves survival in mice
570 with acetaminophen toxicity. In: Gastroenterology. United States. 2007. 132**:** 372-383.
571 Vaquero J and Butterworth RF Mild hypothermia for the treatment of acute liver failure--what are we
572 waiting for? In: Nat Clin Pract Gastroenterol Hepatol. England. 2007. 4**:** 528-529.
573 Zhou J, Empey PE, et al. Cardiac arrest and therapeutic hypothermia decrease isoform-specific
574 cytochrome P450 drug metabolism. Drug Metab Dispos 2011; 39 (12): 2209-2218.
575 Zhou J and Poloyac SM. The effect of therapeutic hypothermia on drug metabolism and response:
576 cellular. Expert Opin Drug Metab Toxicol 2011; 7 (7): 803-816.

577 Zhou SF. Structure, function and regulation of P-glycoprotein and its clinical relevance in drug
578 disposition. Xenobiotica 2008; 38 (7-8): 802-832.
579 Zhuang W, Jia Z, et al. The mechanism of the G0/G1 cell cycle phase arrest induced by activation of
580 PXR in human cells. Biomed Pharmacother 2011; 65 (7): 467-473.
581
582
583

584 **Tables**

585

586 **Table 1: List of 23 target genes related to liver functions (drug metabolism and drug**
587 **transporters) studied using the RealTime ready probes from Roche.**

588

589 **Table 2 : Effects of hypothermia and 3-methylchorentrene on the level of mRNA**
590 **expressions of AhR related genes (*CYP1A2*, *GSTA2*, *UGT1A6*).** Primary rat hepatocytes are
591 cultivated in normo and hypothermia after 72h of induction with 3MC in IDCCM. RTqPCR
592 were performed at Day 2 and Day 4 (after 72h of perfusion). Results are expressed as %
593 compared to the levels in post-extracted rat hepatocytes (Day 0) or at Day 4 (without
594 induction) (mean ± SEM). Data are representative of two separate experiments (N=3 for each
595 experiment) and statistics were performed to detect significant differences between 37 and
596 32°C. ** $P<0.01$, * $P<0.05$.

597

598

599

600

601 **Figure Legends**

602

603 **Figure 1** : **Description of the biochip included in parallel microfluidic box named the**
604 **IDCCM** : (A) PDMS biochip, (B) a view of microchannels, (C) dimension details of
605 microchannels and (D) two IDCCMs connected to the peristaltic pump with 24 PTFE tubes.
606 Corresponding bars were indicated in views A, B & C.

607

608 **Figure 2 : Morphology of primary rat hepatocytes cultivated in normo and hypothermia**
609 **after 72h of perfusion in IDCCM.** (A) Hepatocytes cultivated at 37°C (A) and at 32° (B).
610 Observations under phase microscope evidenced cell morphology with a typical cuboid shape.

611

612 **Figure 3 : Cytoskeleton of primary rat hepatocytes cultivated in normo and**
613 **hypothermia after 48h of perfusion in IDCCM.** Double staining of the actin filaments
614 (rhodamine-phalloidin®) and the cell nucleus Dapi was performed in the biochip cultivated at
615 37°C (**A to C**) and at 32°C (**D to F**). No difference was observed. Immunostaining of actin
616 filaments (**A** and **D**), Dapi (**B** and **E**), overlay of fluorescence views (**C** and **F**). Corresponding
617 bars were indicated in all views.

618

619 **Figure 4** : **Evolution of cell number cultivated in normo and hypothermia during the 72h**
620 **of perfusion in IDCCM.** Mean ± SD of three independent experiments.

621

622 **Figure 5 : Flow cytometry of PI-stained permeabilized primary rat hepatocytes**
623 **cultivated in normo and hypothermia during the 72h of perfusion in IDCCM.** Cell cycle
624 analysis from Day 0 (after hepatocyte extraction) to Day 1 (**A**). Cell cycle analysis from day 2
625 (24h of perfusion) to Day 4 (72h of perfusion) with or without induction experiments (3-

methylcholantren-3MC, rifampicin-RIF) at 37°C (**B**) and 32°C (**C**). The histograms shown are representative of three separate experiments (Mean ± SD) and detailed proportion of G0/G1, S and G2 cells. *** P<0.001, ** P<0.01. In B and C, dotted lines represent the reference level for uninducted cells (no statistical significant).

Figure 6 : Hepatocellular performance of primary rat hepatocytes cultivated in normo and hypothermia during the 72h of perfusion in IDCCM. Glucose consumption (**A**) and albumin secretion (**B**) were analyzed from Day 1 to Day 4 and in induced cell culture (3-methylcholantren-3MC, rifampicin-RIF). The histograms shown are representative of three separate experiments (Mean ± SD). *** P<0.001, ** P<0.01, * P<0.05.

Figure 7 : Mean fold changes in gene expression of primary rat hepatocytes cultivated in normo and hypothermia in IDCCM. RTqPCR were performed at Day 2 (after 24 of perfusion) (**A**) and at Day 4 (after 72h of perfusion) (**B**). The histograms shown are representative of two separate experiments.

Figure 8 : CYP1A2 activity of primary rat hepatocytes cultivated in normo and hypothermia during the 72h of perfusion in IDCCM. Comparison of the resorufin production by 7-ethoxyresorufin O-deethylation (EROD) in uninduced cell cuture from Day 1 to Day 4 (**A**) and in induced cell culture (3-methylcholantren-3MC, rifampicin-RIF) (**B**). The histograms shown are representative of three separate experiments (Mean ± SD). * P<0.05.

Supplemental data:

Table 3: Comparison of the effect of hypothermia on CYP1A2 activity, observed in plate and IDCCM after 48 of culture. The data shown are representative of two (plate) or three (IDDCM) separate experiments.

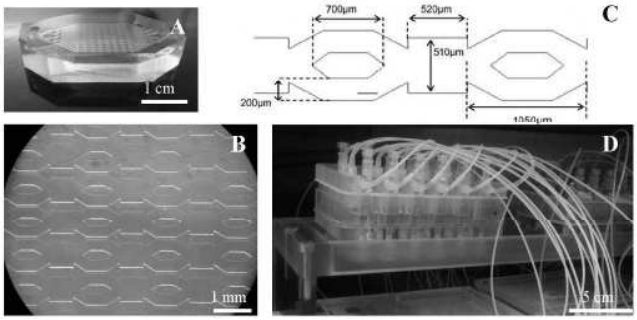

Description of the biochip included in parallel microfluidic box named the IDCCM : (A) PDMS biochip, (B) a view of microchannels, (C) dimension details of microchannels and (D) two IDCCMs connected to the peristaltic pump with 24 PTFE tubes. Corresponding bars were indicated in views A, B & C.
297x210mm (220 x 220 DPI)

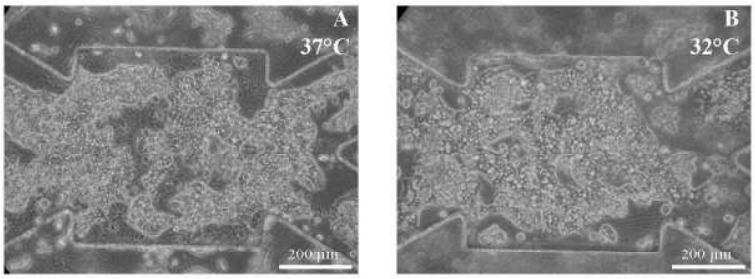

Morphology of primary rat hepatocytes cultivated in normo and hypothermia after 72h of perfusion in IDCCM. (A) Hepatocytes cultivated at 37°C (A) and at 32° (B). Observations under phase microscope evidenced cell morphology with a typical cuboid shape.
297x209mm (217 x 217 DPI)

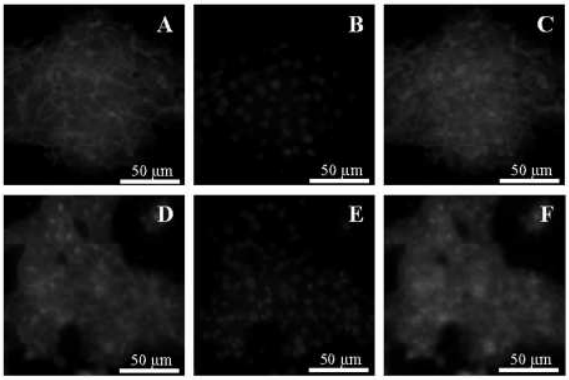

Cytoskeleton of primary rat hepatocytes cultivated in normo and hypothermia after 48h of perfusion in IDCCM. Double staining of the actin filaments (rhodamine-phalloidin®) and the cell nucleus Dapi was performed in the biochip cultivated at 37°C (A to C) and at 32°C (D to F). No difference was observed. Immunostaining of actin filaments (A and D), Dapi (B and E), overlay of fluorescence views (C and F). Corresponding bars were indicated in all views.
297x209mm (120 x 120 DPI)

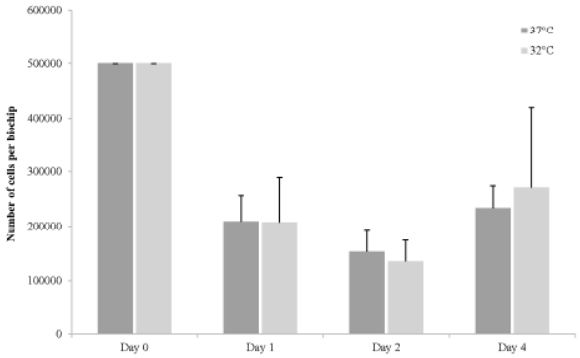

Evolution of cell number cultivated in normo and hypothermia during the 72h of perfusion in IDCCM. Mean ± SD of three independent experiments.
297x209mm (200 x 200 DPI)

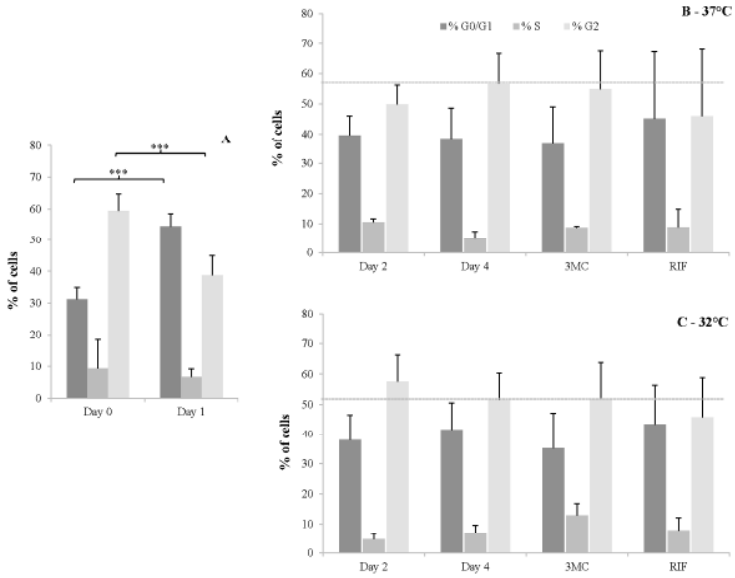

Flow cytometry of PI-stained permeabilized primary rat hepatocytes cultivated in normo and hypothermia during the 72h of perfusion in IDCCM. Cell cycle analysis from Day 0 (after hepatocyte extraction) to Day 1 (A). Cell cycle analysis from day 2 (24h of perfusion) to Day 4 (72h of perfusion) with or without induction experiments (3-methylcholantren-3MC, rifampicin-RIF) at 37°C (B) and 32°C (C). The histograms shown are representative of three separate experiments (Mean ± SD) and detailed proportion of G0/G1, S and G2 cells. *** P<0.001, ** P<0.01. In B and C, dotted lines represent the reference level for uninducted cells (no statistical significant).
297x209mm (200 x 200 DPI)

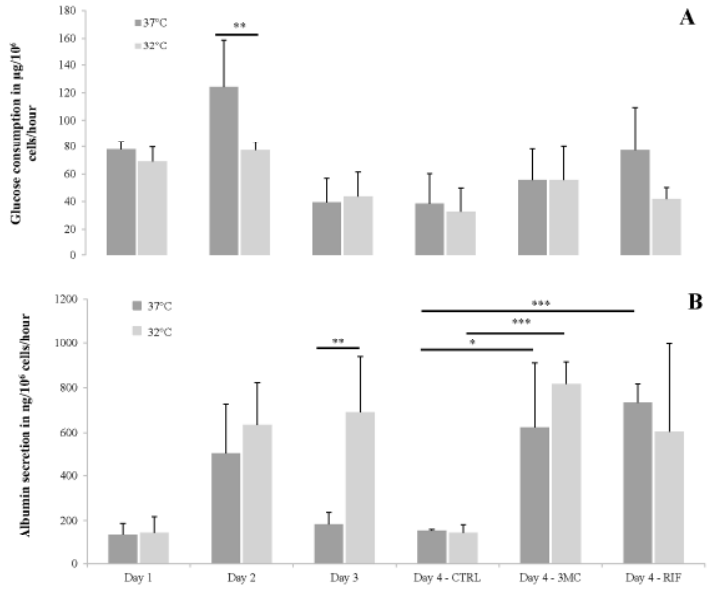

Hepatocellular performance of primary rat hepatocytes cultivated in normo and hypothermia during the 72h of perfusion in IDCCM. Glucose consumption (A) and albumin secretion (B) were analyzed from Day 1 to Day 4 and in induced cell culture (3-methylcholantren-3MC, rifampicin-RIF). The histograms shown are representative of three separate experiments (Mean ± SD). *** P<0.001, ** P<0.01, * P<0.05.
297x209mm (200 x 200 DPI)

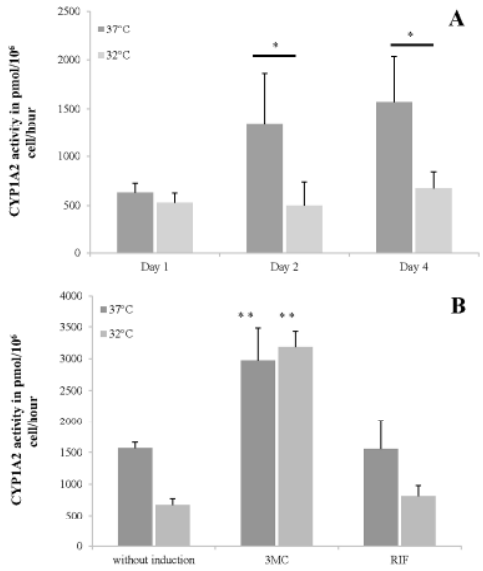

Mean fold changes in gene expression of primary rat hepatocytes cultivated in normo and hypothermia in IDCCM. RTqPCR were performed at Day 2 (after 24 of perfusion) (A) and at Day 4 (after 72h of perfusion) (B). The histograms shown are representative of two separate experiments.
297x209mm (200 x 200 DPI)

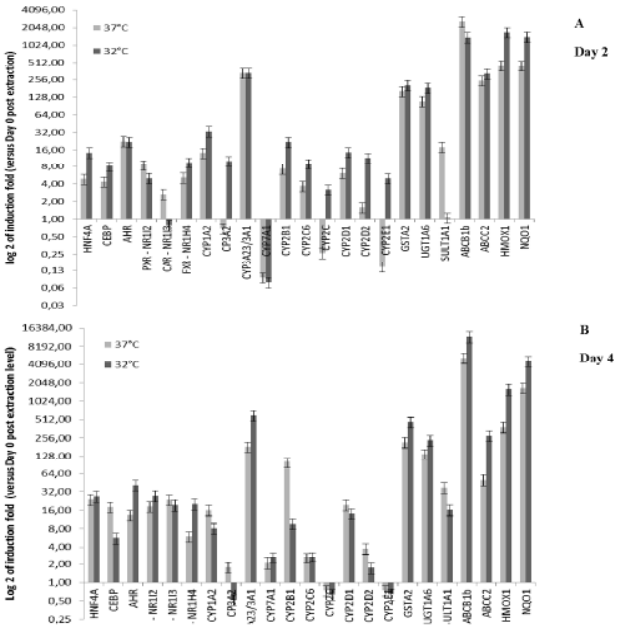

CYP1A2 activity of primary rat hepatocytes cultivated in normo and hypothermia during the 72h of perfusion in IDCCM. Comparison of the resorufin production by 7-ethoxyresorufin O-deethylation (EROD) in uninduced cell cuture from Day 1 to Day 4 (A) and in induced cell culture (3-methylcholantren-3MC, rifampicin-RIF) (B). The histograms shown are representative of three separate experiments (Mean ± SD). * P<0.05.
297x209mm (177 x 177 DPI)

Functions	*Gene Symbol*	Assay ID (RTR)	Amplicon Size (pb)	Accession ID
Hepatic Transcription factors	*HNF4a*	500286	92	ENSRNOT00000011978
	CEBP	503796	112	ENSRNOT00000030773
Xenosensors	*AHR*	503494	73	ENSRNOT00000006618
	PXR - NR1I2	503757	95	ENSRNOT00000003934
	CAR – NRI3	503790	95	ENSRNOT00000049873
	FXR - NR1H4	503760	92	ENSRNOT00000009910
CYPs	*CYP1A2*	503414	60	ENSRNOT00000058571
	CYP3A2	503762	82	ENSRNOT00000001291
	CYP3A23/3A1	502664	65	ENSRNOT00000051244
	CYP7A1	503785	78	ENSRNOT00000012819
	CYP2B1	503749	61	ENSRNOT00000047540
	CYP2C6	503746	96	XM_001066767
	CYP2C	502669	94	ENSRNOT00000017310
	CYP2D1	503742	83	ENSRNOT00000050002
	CYP2D2	503737	60	ENSRNOT00000012413
	CYP2E1	503000	61	ENSRNOT00000016883
Phase II Enzymes	*GSTA2*	502674	78	ENSRNOT00000044944
	SULT1A1	503770	76	ENSRNOT00000026186
	UGT1A6	503773	96	NM_001039691
ABC transporters	*Pgp - ABCB1b*	502651	69	ENSRNOT00000037712
	MRP2- ABCC2	503769	64	NM_012833
Oxidative stress - Inflammation	*HMOX1*	502648	71	ENSRNOT00000019192
Oxidative stress	*NQO1*	502688	77	ENSRNOT00000017174

Gene Symbol	Temperature	Day 2 *versus* Day 0	Day 4 *versus* Day 0	3MC *versus* Day 4
AhR	37°C	22.3 ± 0.9	13.3 ± 0.2	588.7 ± 0.8
	32°C	22.2 ± 1.7	41.3 ± 0.4**	117.7 ± 0.2**
CYP1A2	37°C	14.3 ± 0.4	16.2 ± 0.7	153.4 ± 1.1
	32°C	33.6 ± 0.8*	8.1 ± 0.4*	145.1 ± 1.1*
GSTA2	37°C	163.4 ± 0.2	220.2 ± 0.8	104.4 ± 0.9
	32°C	206.8 ± 2.6**	236.2 ± 0.8	279.4 ± 2.3**
UGT1A6	37°C	109.6 ± 0.1	137.3 ± 0.3	191.5 ± 0.6
	32°C	185.4 ± 0.2*	239.5 ± 0.6**	409.1 ± 1.4**

	Plate		IDDCM	
	37°C	32°C	37°C	32°C
CYP1A2 pmol/10^6cell/h	59±10	44±7	1348±512	500±241